

Scaffold oriented synthesis. Part 2: Design, synthesis and biological evaluation of pyrimido-diazepines as receptor tyrosine kinase inhibitors

Vijaya Gracias, Zhiqin Ji, Irini Akritopoulou-Zanze,* Cele Abad-Zapatero, Jeffrey R. Huth, Danying Song, Philip J. Hajduk, Eric F. Johnson, Keith B. Glaser, Patrick A. Marcotte, Lori Pease, Nirupama B. Soni, Kent D. Stewart, Steven K. Davidsen, Michael R. Michaelides and Stevan W. Djuric

Global Pharmaceutical Research and Development, Abbott Laboratories, 100 Abbott Park Road, Abbott Park, IL 60044, USA

Received 14 January 2008; revised 5 March 2008; accepted 6 March 2008

Available online 10 March 2008

Abstract—We report the discovery of the pyrimido-diazepine scaffolds as novel adenine mimics. Structure-based design led to the discovery of analogs with potent inhibitory activity against receptor tyrosine kinases, such as KDR, Flt3 and c-Kit. Compound **14** exhibited low nanomolar KDR enzymatic and cellular potencies ($IC_{50} = 9$ and 52 nM, respectively). © 2008 Elsevier Ltd. All rights reserved.

Protein kinases have proven to be attractive targets for a variety of therapeutic indications¹ and several kinase inhibitors have progressed to become marketed drugs, particularly for cancer.² All kinases possess a structurally conserved catalytic domain that binds ATP³ and most kinase research programs target this ATP binding site with structurally related adenine mimics. Consequently, many patents have been filed around similar or in many cases identical chemotypes resulting in a congested intellectual property situation.

We have recently reported on our efforts to enhance the Abbott compound collection with novel kinase inhibitors;

an effort intended to help address the above patent challenge.⁴ We have placed an emphasis on the novelty of the designed chemotypes and attempted to create structures that have never been described in patents or in published literature as kinase inhibitors. Specifically, we were interested in identifying novel adenine replacements that upon further functionalization would furnish proprietary kinase inhibitors.

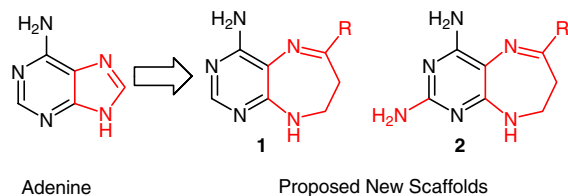
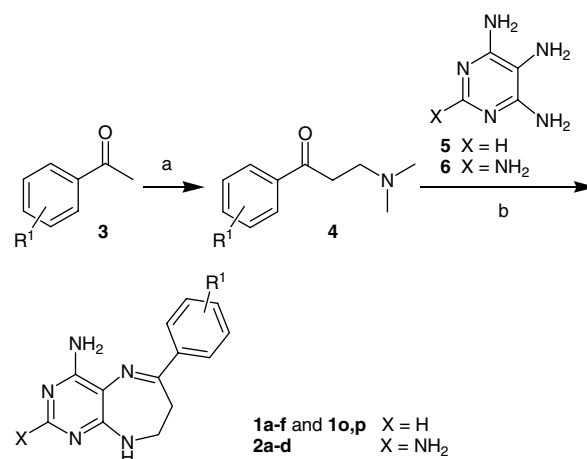


Figure 1. De-novo design of pyrimido-diazepines.

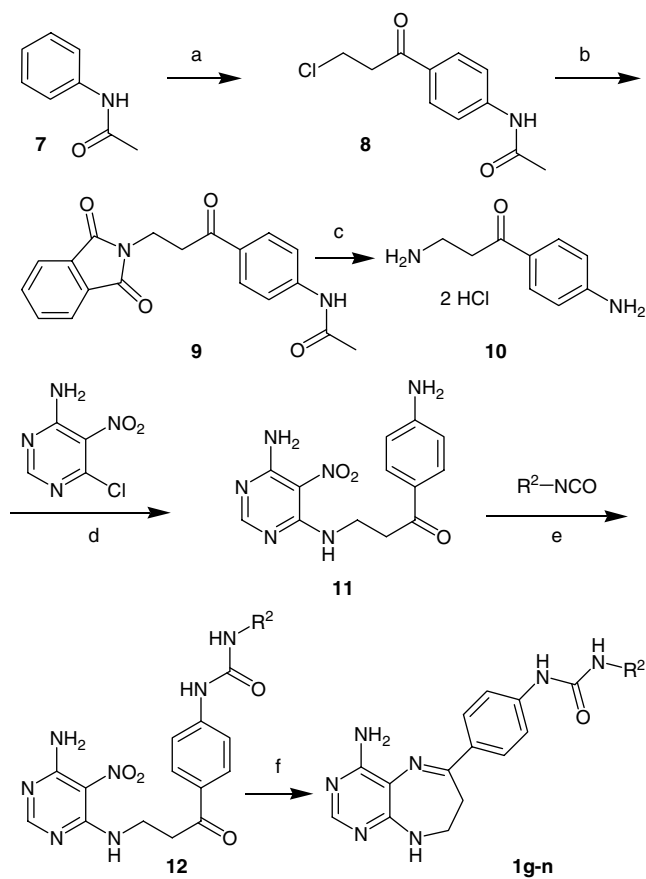
Keywords: KDR inhibitors; VEGFR; PDGFR; cKit inhibitors; Flt3 inhibitors; Adenine mimics; Structure-based drug design.

* Corresponding author. Tel.: +1 847 935 5006; fax: +1 847 935 0310; e-mail: irini.zanze@abbott.com



Scheme 1. Reagents and conditions: (a) Eschenmosher's salt, MeCN, 80 °C, >20%; (b) EtOH, reflux, 1–14%.

In this context we have explored the idea of replacing the imidazole ring of adenine with a seven-membered ring diazepine as shown in Figure 1. We hypothesized that the new pyrimido-diazepine scaffold **1** would bind



Scheme 2. Reagents and conditions: (a) 3-Chloropropanoyl chloride, AlCl_3 , CS_2 , 64%; (b) potassium phthalimide, DMF, 125 °C, 59%; (c) HCl/HOAc , reflux, 72%; (d) Et_3N , 0–75 °C, 83%; (e) DMF, 56%; (f) SnCl_2 , EtOH, 40–70%.

to the hinge region of the target kinase in a manner similar to that exhibited by adenine with the formation of two key hydrogen bond donor/acceptor interactions. We anticipated that additional functionalization of the molecule based on molecular modeling considerations would allow us to explore various sites with the expectation of gains in potency and selectivity depending on the kinase targeted. To exploit the potential of a third hydrogen bond in the hinge region, we designed scaffold **2** which possess an additional amino group in the 2-position of the pyrimidine ring.

The molecules were initially synthesized following previously described procedures.⁵ Reactions of ketones **3** (Scheme 1) with Eschenmosher's salt yielded intermediates **4** which were isolated and subsequently subjected to heating with commercially available pyrimidine-4,5,6-triamines **5** or **6** to provide the pyrimidoazepines **1** or **2**, respectively, in low overall yields.

Subsequently, for the synthesis of more complex analogs, a new synthetic protocol was devised as shown in Scheme 2. Friedel–Crafts acylation of protected aniline **7** with 3-chloropropanoyl chloride provided precursor **8**, which was subjected to nucleophilic substitution with potassium phthalimide to yield compound **9** in good yield. Acid deprotection of both amino groups of **9** provided **10** as the diacid salt in good yield. Nucleophilic aromatic substitution of 6-chloro-5-nitropyrimidin-4-amine with **10** in the presence of triethylamine furnished compound **11**. At this point various isocyanates were reacted with aniline **11** to yield exclusively ureas **12**. Final compounds **1** were obtained upon reduction of the nitro group and spontaneous imine formation of the resulting amine with the carbonyl group of **12**.

Initially, simple analogs of **1** and **2** were tested against a preliminary panel of five kinases of interest^{4,6} at low concentration of ATP (10 μM) in order to detect even

Table 1. Kinase inhibitory activity of pyrimido-diazepine analogs **1** and **2** against an exploratory kinase panel

Compound	X	R ¹	KDR IC ₅₀ ^a (μM)	Plk1 IC ₅₀ ^a (μM)	Pak4 IC ₅₀ ^a (μM)	CK2 IC ₅₀ ^a (μM)	Akt1 IC ₅₀ ^a (μM)
1a	H	H	3 ^b	>100	>100	4 ^b	92
1b	H	3-Me	3	50	>100	12	>100
1c	H	4-Me	4	>100	>100	>100	>100
1d	H	3-Cl	0.6	>100	>100	64% ^c	>100
1e	H	4-Cl	3	>100	>100	>100	>100
2a	NH ₂	H	35	>100	>100	>100	>100
2b	NH ₂	3-Cl	21	>100	>100	21	>100
2c	NH ₂	4-Cl	9	>100	>100	>100	>100

^a IC₅₀ values are based on an eleven point curve at 10 μM ATP concentration, >100 indicates less than 50% inhibition at that concentration or an IC₅₀ > 100 μM .

^b Average of two values.

^c Indicates % inhibition at 100 μM .

weak inhibitory activity trends. Most of the analogs exhibited modest activity against KDR in the single digit micromolar and high submicromolar range and some were active against CK2 (Table 1). The presence of the extra amino group in analogs **2** had a negative effect

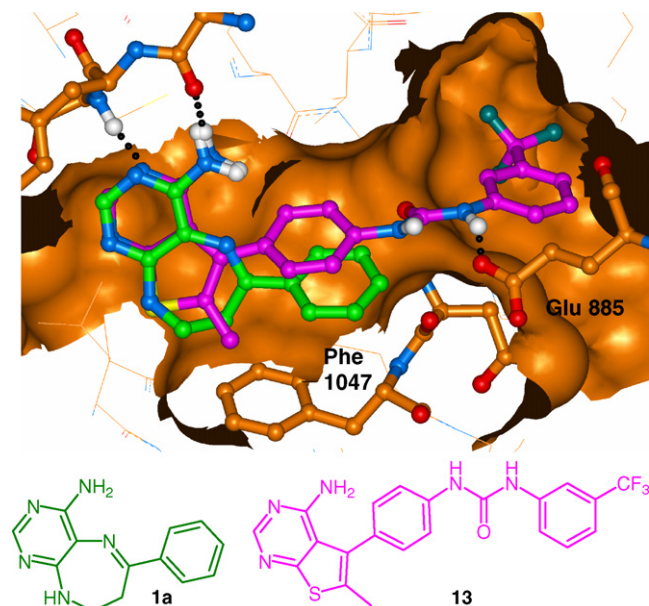


Figure 2. Model of compound **1a**, green carbons, bound to KDR kinase in ‘inactive’ conformation with Phe 1047 in the DFG-out position [model created as in Refs. 7 and 10]. Hinge hydrogen bonds to the backbone Glu 917 C=O and Cys 917 N–H are shown with black dotted lines. A model of thienopyrimidine KDR inhibitor previously published⁷ is shown with pink carbons and with its urea H-bond to Glu 885.

on the KDR inhibitory activity of the compounds (**1a** vs **2a**, **1d** vs **2b**, and **1e** vs **2c**).

Encouraged by these initial results we decided to further investigate the KDR inhibitory potency of the series by employing molecular modeling. Superimposition of plain compound **1a** with previously reported KDR inhibitor **13**⁷ (Fig. 2) provided us with insights as to how to best take advantage of the hydrophobic ‘back pocket’ of KDR. Introduction of urea functionality such as in **13** has been shown to have beneficial effects on KDR inhibitory activity (KDR IC₅₀ = 52 nM) and such compounds have been part of a program at Abbott aiming to develop PDGFR and VEGFR multitargeted kinase inhibitors.^{7–10}

Based on modeling considerations, both *para*- and *meta*-positions of the phenyl ring provided reasonable vectors to extend the urea functionality. We selected to prepare a small group of key urea analogs to validate our modeling hypothesis. The urea analogs were synthesized according to Schemes 1 and 2 from the appropriate starting materials and tested against KDR, Flt3, and c-Kit in an HTRF assay format at 1 mM ATP.

We immediately observed an improvement in KDR potency with the simple *para*-phenyl urea analog **1f** (Table 2) in comparison to **1a**. However, its 2-amino analog equivalent **2d** was not active under the assay conditions and these analogs were not further pursued. Introduction of a trifluoromethyl group in the *meta*-position of the urea phenyl ring (compound **1g**) dramatically increased the *in vitro* KDR potency. **1g** was also very potent against Flt3 and c-Kit and in the KDR cellular assay. The presence of the same group in the *para*-posi-

Table 2. Kinase inhibitory activity of *para*-urea analogs **1** and **2**

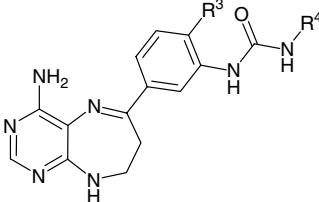
Compound	X	R ²	KDR IC ₅₀ ^a (μM)	KDR (cell) ^b IC ₅₀ ^c (μM)	Flt3 IC ₅₀ ^a (μM)	c-Kit IC ₅₀ ^a (μM)
1f	H	Ph	0.951	ND ^d	ND	ND
2d	NH ₂	Ph	>13	ND	2.858	>13
1g	H	3-CF ₃ -Ph	0.003	0.013	0.002	0.006
1h	H	4-CF ₃ -Ph	0.110	2.440	0.009	0.035
1i	H	3-Cl-Ph	0.019	0.050	0.006	0.018
1j	H	2-F-3-CF ₃ -Ph	0.049	1.520	0.003	0.028
1k	H	4-F-3-CF ₃ -Ph	0.005	0.345	0.007	0.022
1l	H	4-Cl-3-CF ₃ -Ph	0.006	0.049	0.016	0.050
1m	H	2-F-5-Me-Ph	0.065	0.311	0.013	0.037
1n	H	2-F-5-CF ₃ -Ph	0.004	0.121	0.002	0.011

^a IC₅₀ values are based on an eleven point curve at 1 mM ATP concentration.

^b Activity against VEGF-induced KDR phosphorylation in 3T3-murine fibroblast cells.

^c Average of two experiments.

^d ND stands for not determined.

Table 3. Kinase inhibitory activity of meta-urea analogs


Compound	R ³	R ⁴	KDR IC ₅₀ ^a (μM)	KDR (cell) ^b IC ₅₀ (μM)	Flt3 IC ₅₀ ^a (μM)	c-Kit IC ₅₀ ^a (μM)
1o	H	Ph	0.888	ND ^c	2.696	3.022
1p	H	3-CF ₃ -Ph	0.126	0.790	0.145	0.091
14	Me	3-CF ₃ -Ph	0.006	0.052	0.135	0.012

^a IC₅₀ values are based on an eleven point curve at 1 mM ATP concentration.

^b Activity against VEGF-induced KDR phosphorylation in 3T3-murine fibroblast cells.

^c ND stands for not determined.

tion (**1h**) resulted in losses in KDR potency. Di-substituted analogs containing the *meta*-trifluoromethyl group and a fluoro group in various positions resulted in compounds with similar in vitro KDR potency, (**1k** and **1l**) however, their cellular potency was inferior to that of compound **1g**.

The *meta*-substituted phenyl urea **1o** (Table 3) exhibited a similar drop in potency when compared to **1a**. However, the *meta*-trifluoromethyl phenyl analog of the *meta*-urea **1p** was not as potent as **1g**. Modeling of **1p** in the active site of KDR (Fig. 3) suggested the presence of a small pocket that could be filled with additional functionality. Thus compound **14** was prepared following procedures similar to those in Scheme 1. To our delight compound **14** exhibited improved in vitro and cellular KDR potency and an apparent selectivity for KDR versus Flt3 (Table 3). This is in stark contrast to the *para*-urea series (Table 2) where most of the compounds were equipotent for Flt3 and to *meta*-urea analogs such as **1p** lacking the methyl group. The altered KDR/Flt3 enzyme potency ratio for compounds **1p**

and **14** is potentially due to the different gatekeeper residues for the two enzymes, Val 916 for KDR and Phe 691 for Flt3, which is in the direct vicinity of the aryl Me group of **14**.

In conclusion, we have identified pyrimido-diazepines as novel kinase hinge binders and were able to rapidly transform them to potent VEGFR and PDGFR inhibitors using modeling and our expertise in kinase inhibition. We are in the process of finding other applications for this unique core and our findings will be reported in due course.

Acknowledgments

The authors thank the Abbott High Throughput Purification and Structural Chemistry groups for their support with purification and analytical data, respectively.

References and notes

- Akritopoulou-Zanze, I. *Drugs* **2006**, *9*, 481.
- (a) de Cárcer, G.; Pérez de Castro, I.; Malumbres, M. *Curr. Med. Chem.* **2007**, *14*, 969; (b) Schenone, S.; Bondavalli, F.; Botta, M. *Curr. Med. Chem.* **2007**, *14*, 2495; (c) Steeghs, N.; Nortier, J. W. R.; Gelderblom, H. *Ann. Surg. Onc.* **2007**, *14*, 942.
- Liao, J. J.-L. *J. Med. Chem.* **2007**, *50*, 409.
- Akritopoulou-Zanze, I.; Darczak, D.; Sarris, K.; Phelan, K. M.; Huth, J. R.; Song, D.; Johnson, E. F.; Jia, J.; Djuric, S. W. *Bioorg. Med. Chem. Lett.* **2005**, *16*, 96.
- (a) Saitz, C.; Jullian, C. *J. Heterocyclic Chem.* **2000**, *37*, 401; (b) Insuasty, B.; Perez, A.; Valencia, J.; Quiroga, J. *J. Heterocyclic Chem.* **1997**, *34*, 1555.
- Luo, Y.; Smith, R. A.; Guan, R.; Liu, X.; Klinghofer, V.; Shen, J.; Hutchins, C.; Richardson, P.; Holzman, T.; Rosenberg, S. H.; Giranda, V. L. *Biochemistry* **2004**, *43*, 1254.
- Dai, Y.; Guo, Y.; Frey, R. R.; Ji, Z.; Curtin, M. L.; Ahmed, A. A.; Albert, D. H.; Arnold, L.; Arries, S. S.; Barlozzari, T.; Bauch, J. L.; Bouska, J. J.; Bousquet, P. F.; Cunha, G. A.; Glaser, K. B.; Guo, J.; Li, J.; Marcotte, P. A.; Marsh, K. C.; Moskey, M. D.; Pease, L. J.; Stewart, K.

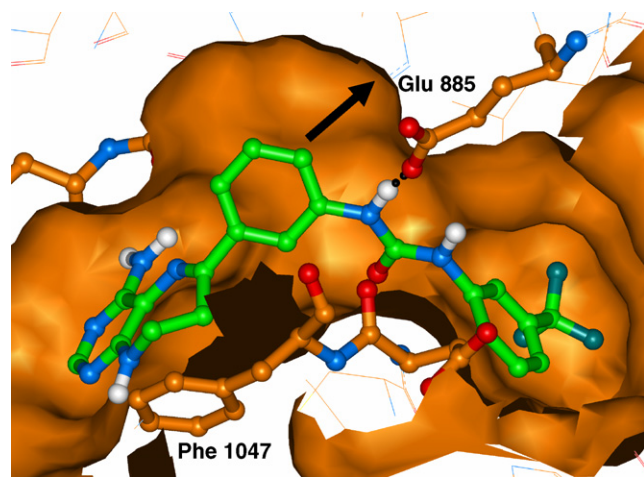


Figure 3. Model of compound **1p**, green carbons, bound to KDR with the urea of **1p** hydrogen-bonded to Glu 885. The arrow shows a vector that projects into a small hydrophobic volume comprising the sidechains of Val 848, Val 916, and the methylenes of Lys 868.

- D.; Stoll, V. S.; Tapang, P.; Wishart, N.; Davidsen, S. K.; Michaelides, M. R. *J. Med. Chem.* **2005**, *48*, 6066.
8. Dinges, J.; Ashworth, K. L.; Akritopoulou-Zanze, I.; Arnold, L. D.; Baumeister, S. A.; Bousquet, P. F.; Cunha, G. A.; Davidsen, S. K.; Djuric, S. W.; Gracias, V. J.; Michaelides, M. R.; Rafferty, P.; Sowin, T. J.; Stewart, K. D.; Xia, Z.; Zhang, H. Q. *Bioorg. Med. Chem. Lett.* **2006**, *16*, 4266.
9. Ji, Z.; Ahmed, A. A.; Albert, D. H.; Bouska, J. J.; Bousquet, P. F.; Cunha, G. A.; Glaser, K. B.; Guo, J.; Li, J.; Marcotte, P. A.; Moskey, M. D.; Pease, L. J.; Stewart, K. D.; Yates, M.; Davidsen, S. K.; Michaelides, M. R. *Bioorg. Med. Chem. Lett.* **2006**, *16*, 4326.
10. Dai, Y.; Hartandi, K.; Ji, Z.; Ahmed, A. A.; Albert, D. H.; Bauch, J. L.; Bouska, J. J.; Bousquet, P. F.; Cunha, G. A.; Glaser, K. B.; Harris, C. M.; Hickman, D.; Guo, J.; Li, J.; Marcotte, P. A.; Marsh, K. C.; Moskey, M. D.; Martin, R. L.; Olson, A. M.; Osterling, D. J.; Pease, L. J.; Soni, N. B.; Stewart, K. D.; Stoll, V. S.; Tapang, P.; Reuter, D. R.; Davidsen, S. K.; Michaelides, M. R. *J. Med. Chem.* **2007**, *50*, 1584.